COBEM 2023 27TH INTERNATIONAL CONGRESS OF MECHANICAL ENGENEERING

ABCM Brazilian Society of Mechanical Sciences and Engineering
27th ABCM International Congress of Mechanical Engineering
December 04-08, 2023, Florianópolis-SC, Brazil

COB-2023-0745
EXPERIMENTAL STUDY AND MODELING OF A $H_2O/NH_3/H_2$ SOLAR DIFFUSION-ABSORPTION REFRIGERATOR FOR VACCINE STORAGE IN REGIONS WITHOUT ELECTRIFICATION

Gustavo Sana Trindade
Willian Moreira Duarte
Graduate Program in Mechanical Engineering – Universidade Federal de Minas Gerais, Av. Antônio Calor, 6627, Belo Horizonte, MG, CEP: 31.270-901
gsannat@ufmg.br willian@demec.ufmg.br

Fabiano Drumond Chaves
Department of Computing and Mechanics - Centro Federal de Educação Tecnológica, Rua José Peres, 558, Leopoldina, MG, CEP:36.700-000
fabianodc@cefetmg.br

Nathália Beatriz Amorim Santos
Mechanical Engineering Undergraduate - Universidade Federal de Minas Gerais, Av. Antônio Calor, 6627, Belo Horizonte, MG, CEP: 31.270-901
nathbas011@gmail.com

Luiz Machado
Graduate Program in Mechanical Engineering – Universidade Federal de Minas Gerais, Av. Antônio Calor, 6627, Belo Horizonte, MG, CEP: 31.270-901
luizm@ufmg.br

Abstract. *The objective of this work is to present a distributed condenser steady state mathematical model, written in Python language, of a $H_2O/NH_3/H_2$ diffusion and absorption fridge for vaccine storage in regions without electrification. The refrigerator thermal input in ammonia vapor generator set was originally promoted by Joule effect through an 80.7 W electrical resistance. To supply the system with solar energy, the resistor is going to be replaced by a coaxial heat exchanger, in which thermal oil heated in a solar concentrator flows in annular space of the outer tube. Condenser, generator and rectifier models were based on the energy, mass balance equations applications for ammonia and water and the energy balance equation application for heat exchangers walls. Condenser input variables were obtained through peripheral components models. Thus, the ammonia mass flow rate and enthalpy at condenser inlet derive from generator set model, as well as the output mass flow rate resulting from Bernoulli's equation application, corrected for viscous effects, for ammonia flow along the pipe that connects condenser and evaporator. Total system operating pressure that does not vary spatially is the main model output variables. This variable is the result of a series of convergences involving model's equations, one of which is based on ammonia flows equality at condenser inlet and outlet. Model simulations carried out revealed that total single pressure is equal to 1477000 Pa (14.77 bar). In addition, the ammonia, ammonia/water solution, and wall temperature profiles were determined for these components. Finally, the model was validated by comparing the calculated values and the experimental data obtained by measurements performed with thermocouples and infrared thermography. Differences between theoretical and experimental values were a maximum of 6.1%.*

Keywords: *Diffusion absorption refrigerator, Solar energy, Modeling, Vaccine storage, Heat transfer*

1. INTRODUCTION

Intensive vaccination programs are essential in Brazil and worldwide to maintain public health, but the lack of electricity access is one of the underlying reasons that prevent vaccines from being received in many remote areas (Uddin *et al.*, 2021). According to the IEA (2022), 774 million people haven't had access to electricity in 2022, which hundreds of thousands are Brazilian (Alvala *et al.*, 2019). Therefore, a solar cooler could be a solution for storing and transporting vaccines and medicines to these areas, many of which have high solar irradiation rates, such as Brazilian northern region. To assess the applicability of this alternative, a thermal system mathematical modeling is essential to predict the cooler behavior and provide an algorithm to control inside vaccines temperature.

The diffusion-absorption refrigerator (DAR), invented by the Swedes Von Platen and Munters, is a suitable system

for the present application because it does not involve moving components as compressors in traditional refrigeration machines and the power source can be independent of electricity. These machines can operate with thermal renewable energy like solar source and generally operate with ammonia as coolant, a natural fluid with low global warming potential (GWP). For these reasons, many researchers investigate this type of system.

In this context, Chaves *et al.* (2019) developed a model of a conventional commercial DAR and validated it experimentally. The results were satisfactory and the work contributed to a better understanding of the chiller thermodynamic behavior in steady state regime. Pérez-García *et al.* (2019) presented a similar model with less input data and the results were also in agreement with experimental results, which 8% was the maximum COP relative error, as obtained by Mansouri *et al.* (2017) who also developed a dynamic black-box model to correlate generator power input to refrigerator cooling capacity. Moreira (2014), on the other hand, has developed a white box dynamic model that showed regular predictive ability for transient period determination.

Some adaptations for DAR operation with other energy sources also attracted researchers. Vasconcellos (2019) in his doctoral thesis evaluated the energy efficiency of a DAR driven by the exhaust gases of an internal combustion engine and he has concluded that the proposed model allowed thermodynamic properties evaluation along system components, but it demands more experimental data to improve it and validate it.

With respect to solar thermal input, Schmid *et al.* (2019) recently develop a demonstration plant of a solar-driven $H_2O/NH_3/H_2$ diffusion absorption chiller and obtained considerably efficiency and cooling capacity improvement.

Based on the foregoing, the objective of the this work is to present a steady state mathematical model of the condenser of a commercial $H_2O/NH_3/H_2$ DAR manufactured by Dometic and the experimental validation performed. This model, written in Python language, depends on the downstream and upstream models. So, the generator and the condenser/evaporator connecting component models are also elaborated. In addition to coolant and wall temperature profiles, this integration provided the system's total operating pressure, an indispensable parameter for modeling the whole system that contains a parabolic trough collector to heat a thermal oil that will exchange heat with ammonia/water solution instead of heating provided conventionally by an electrical resistance. Figure 1 illustrates the proposed system.

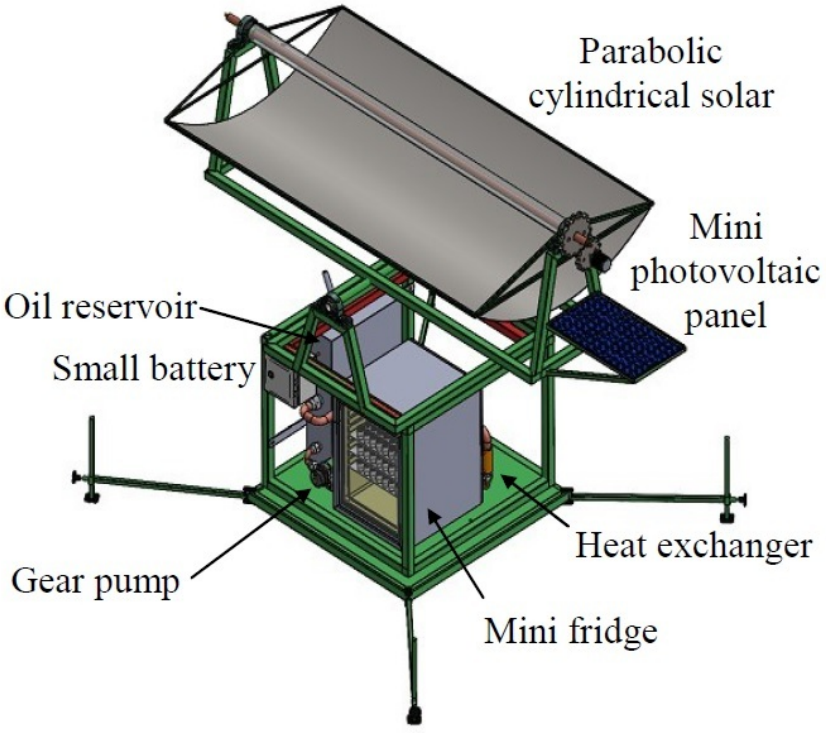

Figure 1: Solar DAR for vaccine storage.

2. METHODOLOGY

2.1 Cycle description

A DAR schematic cycle is shown in Fig. 2, adapted from Choi *et al.* (2022). In generator heat is supplied to ammonia/water solution and the resulting vapor which is mainly composed by ammonia rises due the buoyancy force. Rich solution goes to rectifier whose function is to condensing the remaining water. Some ammonia condensation also can

occur in rectifier. After full water condensation, pure ammonia can cool down in remaining rectifier length before it enters in condenser, where there may be total or partial ammonia vapor condensation. If there is remaining steam, it is directed to a gas heat exchanger (GHX) through a tube not shown in Fig. 2. So the liquid coolant moves to evaporator owing to gravity, where a lot of gas helium is present that has passed through absorber and enters in evaporator through GHX. Consequently, liquid ammonia partial pressure rapidly decreases when it enters in evaporator. The function of helium gas in the system is precisely to induce this drop in ammnia partial pressure so that evaporation, and consequently, the production of cold, can occurs. In sequence, vaporized ammonia is absorbed into weak solution coming in counter flow from a solution heat exchanger (SHX), required to increase mixture potential energy coming from generator's annular region and enable its entrance in absorber. The present mathematical modeling focuses on four components: generator, rectifier, condenser/evaporator tube also namely siphon and condenser. Sequently, instrumental validation has been done through thermocouples installation and infrared thermography.

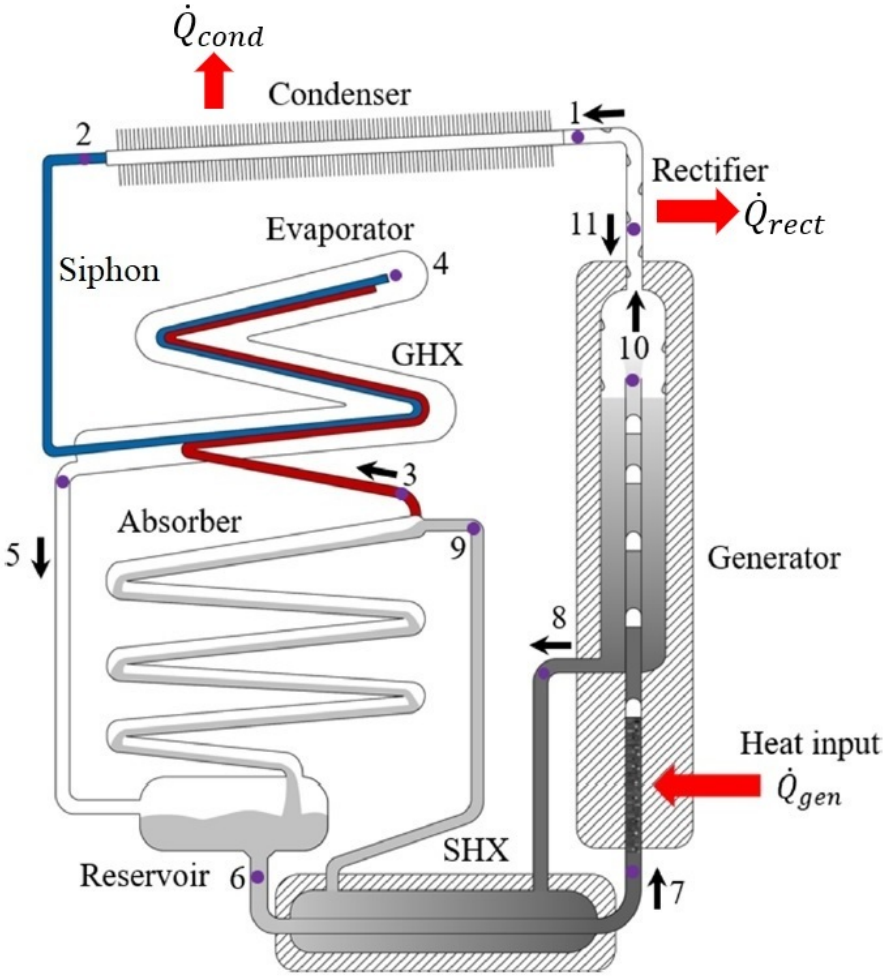

Figure 2: DAR schematic cycle.

2.2 Mathematical modeling

2.2.1 Generator and rectifier models

The library of thermodynamic functions for ammonia-water mixture is available in Engineering Equation Solver (EES). With ammonia mass concentration and pressure, for example, temperature and the other properties are obtained for liquid or vapor phases. So an EES program was elaborated to model generator and rectifier. Both components must be modeled together so that the number of equations equals the number of unknowns variables. The desired output variables of this joint model are the condenser input mass flow rate ($\dot{m}_1$) and input enthalpy (h_1), both as pressure functions. These functions can be obtained by EES curve fit given by graphs constructed from parametric tables, which determine how interest variables vary as system pressure also varies. The input variables were: outer rectifier diameter ($D_{rectext}$), inner rectifier diameter ($D_{rectint}$), heat input ($\dot{Q}_{gen}$), rectifier length (L_{rect}), atmospheric pressure (P_{atm}), ambient temperature (T_{amb}), emissivity (ϵ), input ammonia mass concentration (x_7), and input mass flow rate ($\dot{m}_7$). The latter two generator

input variables are obtained from the model of prior generator component. The model considerations were: generator is insulated, so there are no heat losses; linear variation of mass concentration along rectifier; only water condenses in rectifier, because at typical DAR operation pressures ammonia condensation temperature is lower than those in question; wall temperature equals liquid water that condenses along rectifier and pressure drop negligible. Generator steady state balances of energy, global mass and ammonia mass are given by Eq. (1), Eq. (2) and Eq. (3), respectively.

$$\dot{Q}_{gen} + \dot{m}_7 h_7 + \dot{m}_{11} h_{11} - \dot{m}_8 h_8 - \dot{m}_{10} h_{10} = 0 \tag{1}$$

$$\dot{m}_{11} + \dot{m}_7 - \dot{m}_8 - \dot{m}_{10} = 0 \tag{2}$$

$$\dot{m}_7 x_7 - \dot{m}_8 x_8 - \dot{m}_{10} x_{10} = 0 \tag{3}$$

h, x and $\dot{m}$ are enthalpy, mass concentration and mass flow rate, respectively. The subscribed numbering is according with spatial convention shown in Fig. 2.

Rectifier steady state internal balances of energy, global mass and ammonia mass are given by Eq. (4), Eq. (5) and Eq. (6), respectively.

$$-\dot{Q}_{rect} + \dot{m}_{10} h_{10} - \dot{m}_{11} h_{11} - \dot{m}_1 h_1 = 0 \tag{4}$$

$$\dot{m}_{10} - \dot{m}_{11} - \dot{m}_1 = 0 \tag{5}$$

$$\dot{m}_{10} x_{10} - \dot{m}_1 = 0 \tag{6}$$

$\dot{Q}_{rect}$ represents heat that coming out from rectifier and it can also be modeled from internal and external heat transfer equations, Eq. (7) and Eq. (8), respectively.

$$\dot{Q}_{rect} = \frac{1}{R_{int}}(T_{int} - T_w) \tag{7}$$

$$\dot{Q}_{rect} = \frac{1}{(R_{ext} + R_{rad})}(T_w - T_{amb}) \tag{8}$$

T_w represents wall temperature. R_{ext}, R_{int} and R_{rad} represent external convection, internal thermal and radiation resistances, given by Eq. (9), Eq. (10) and Eq. (11), respectively:

$$R_{ext} = \frac{1}{c_{ext} \pi L_{rect} D_{rectext}} \tag{9}$$

$$R_{int} = \frac{1}{c_{int} \pi L_{rect} D_{rectint}} \tag{10}$$

$$R_{rad} = \frac{1}{c_{rad} \pi L_{rect} D_{rectext}} \tag{11}$$

c_{ext} represents the external natural convection coefficient, given by Churchill and Chu correlation. c_{rad} represents the heat transfer coefficient by radiation, Eq. (12), significant in this case, because wall temperature is significantly higher than ambient temperature.

$$c_{rad} = \varepsilon \sigma (T_w + T_{amb})(T_w^2 + T_{amb}^2) \tag{12}$$

σ equals Stefan–Boltzmann constant.

Two control volumes were used to model rectifier. One which there is water condensation and other which there is ammonia cooling. Thus, L_{rect} is a output variable for each section. In first control volume c_{int} is given by Nusselt laminar correlation, as suggested by Chaves *et al.* (2019). In second control volume c_{int} is given by Nusselt number equals 3.66, considering fully developed laminar flow with constant wall temperature.

2.2.2 Siphon model

Siphon was modeled from Bernoulli's equation corrected for viscous effects for ammonia flow along the pipe that connects condenser and evaporator. The desired output variables is the condenser output mass flow rate ($\dot{m}_2$) as function of pressure and condenser output enthalpy if there is ammonia subcooling. A program in Python language was elaborated and the input variables were: pipe length (L_s), the difference in height between condenser outlet and evaporator inlet (Δz_s), internal siphon diameter (D_s) and the localized pressure drop coefficient (K). The model considerations were: pressure drop and velocity variations are negligible because mass flow rate is constant and the flow is incompressible. Therefore, Bernoulli's equation corrected for viscous effects for siphon is given by Eq. (13).

$$\Delta z_s = \frac{f L_s v^2}{2 D_s g} + \frac{K v^2}{2g} \tag{13}$$

v represents the flow average velocity. Soon, the condenser output mass flow rate as pressure function could be calculated from v. The required specific mass and viscosity are calculated depending on condenser output state. If ammonia comes out subcooled, enthalpy must be provided. It comes from condenser model. Otherwise, there is saturated liquid. f represents the friction factor, function only of Reynolds number because the flow is laminar.

2.2.3 Condenser model

Condenser model was developed in a distributed way in Python language due to ease developing distributed models, i.e. the component is divided into several control volumes. The number of control volumes was determined so that the length of each control volume is of the same order of magnitude as condenser's outer diameter. The model was based on energy balance for the heat exchanger wall, Eq. (14), and on energy and mass balances equations for ammonia, Eq. (15).

$$c_{int} S_{int} (T_{NH3} - T_w) = c_{ext} S_w (Tw - T_{amb}) + c_{ext} S_{fin} \eta_{fin} (Tp - T_{amb}) + c_{rad} S_{ext} (T_w - T_{amb}) \tag{14}$$

$$\dot{m}_1 (h_{in} - h_{out}) = c_{int} S_{int} (T_{NH3} - T_w) \rightarrow h_{out} = \frac{\dot{m}_1 h_{in} - c_{int} S_{int} (T_{NH3} - T_w)}{\dot{m}_1} \tag{15}$$

h_{in} and h_{out} represent input and output ammonia enthalpy for each control volume, respectively. S_{int}, S_{ext}, S_w, S_{fin} represent internal, external, wall and fin areas for each control volume, respectively. η_{fin} and T_{NH3} represent fins efficiency and ammonia temperature for each control volume, respectively.

c_{int} is given by Chato correlation as suggested by Incropera *et al.* (2008) for film condensation inside horizontal tubes. c_{ext} was calculated from Churchill and Chu natural convective correlation.

The desired output variables in condenser is the operation system pressure that does not vary spatially and the condensation heat (Q_{cond}), calculated by Eq. (16).

$$\dot{Q}_{cond} = m_1 (h_2 - h_1) \tag{16}$$

The input variables were: condenser length (L_{cond}) and inclination (θ), internal ($D_{condint}$) and external ($D_{condext}$) condenser diameters, fin efficiency, fin dimensions, number of fins (N_{fin}) and generator and siphon output variables. Accelerational, frictional, and gravitational pressure drops were calculated and it is concluded that its magnitudes are negligible compared to typical operating pressures. A convergence criterion of 5% has been stipulated, i.e. when mass balance is satisfied for a difference of less than 5% the pressure is taken as satisfactory and the model stops calculations. Figure 3 illustrates the full methodology flow chart. q represents the quality.

2.3 Experiment apparatus

Two thermocouples were installed in the present DAR, one in rectifier entrance and other in condenser outlet, as shown in Fig. 4. A third thermocouple was positioned at distance to record ambient temperature. The thermocouples readings, properly calibrated, were recorded using a digital thermometer with a resolution of 0.1°C.

The refrigerator was then turned on and sufficient time was waited for steady state to be established, guaranteed by measurements stabilization. After that, a infrared thermographic measurement with a SC660 FLIR 0.01°C resolution camera was performed to have another comparative basis with the present model. Furthermore, from comparison with thermocouples readings it was possible to calibrate thermographic camera parameters and determine the average surface emissivity, one model's input data.

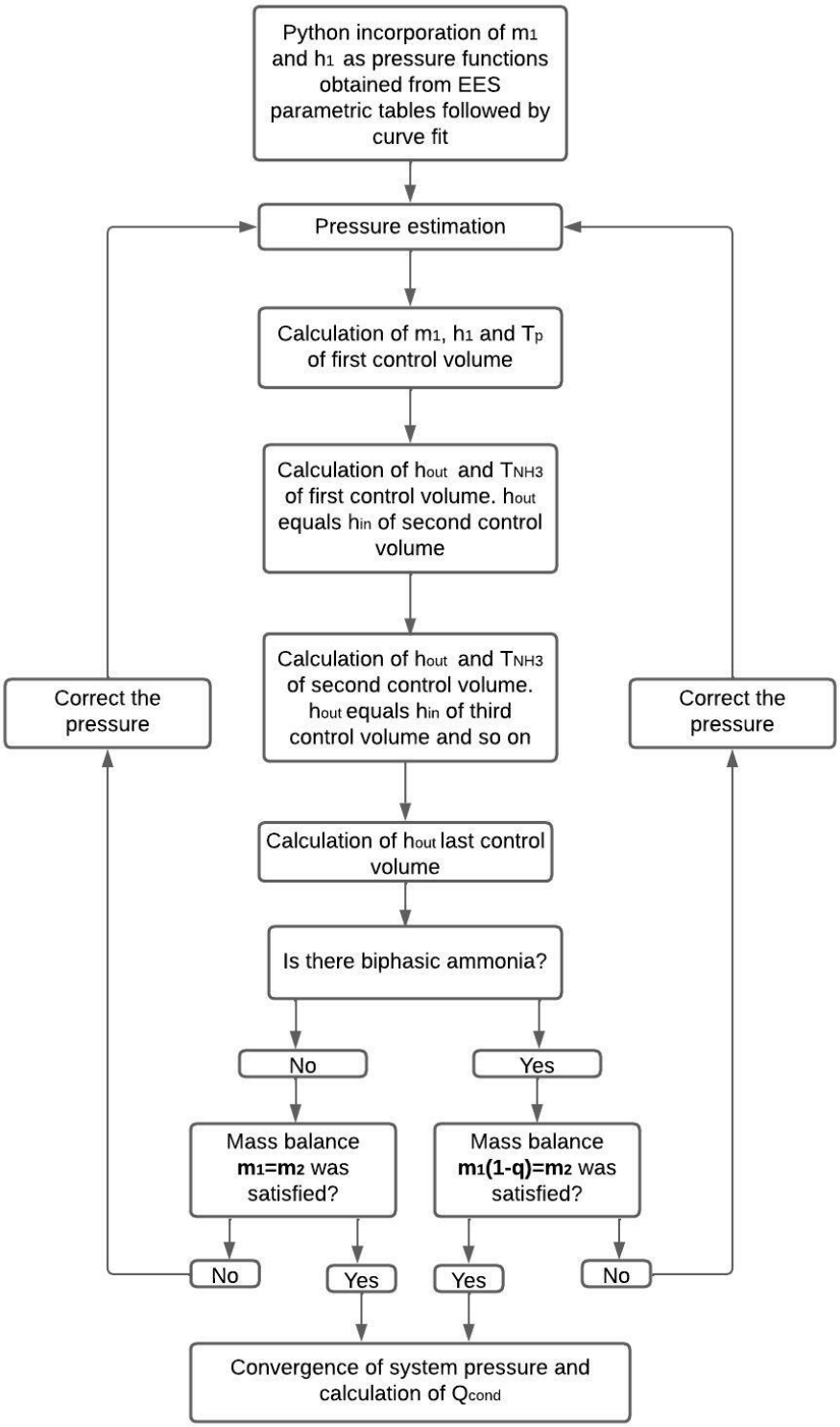

Figure 3: Full methodology flow chart.

3. RESULTS

3.1 Experimental results

Figure 5 shows the thermocouples measurements. On average T_w at rectifier inlet, T_w at condenser outlet and T_{amb} are equal to 392.3 K, 307.5 K and 294.9 K, respectively.

Figure 6 shows the thermographic image. It can be observed from thermographic image that T_w at rectifier inlet, T_w at condenser inlet and T_w at condenser outlet are equal to 392.25 K, 317.49 K and 308.50 K, respectively. Moreover, the

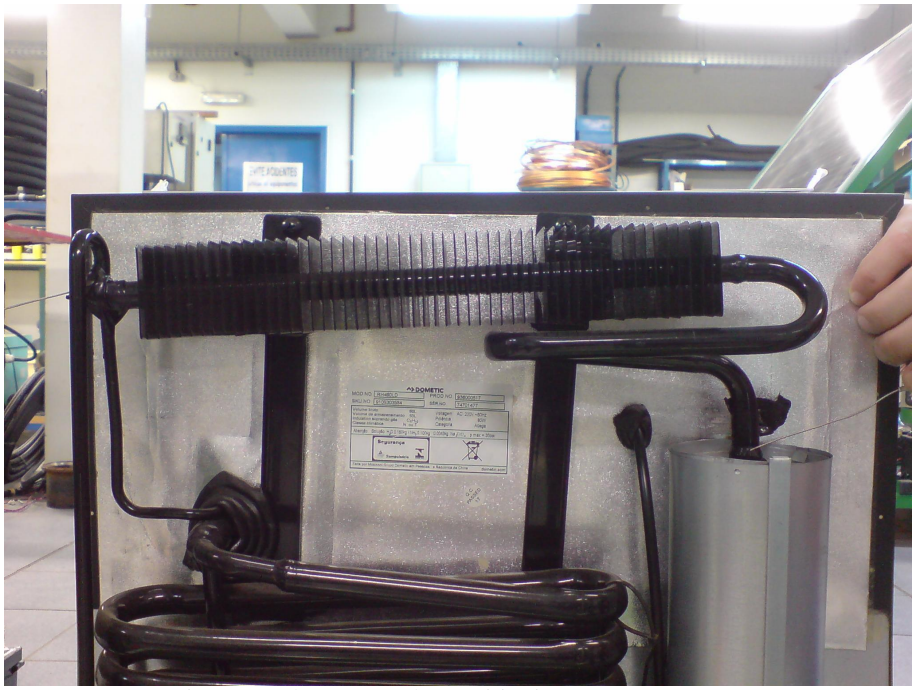

Figure 4: Thermocouples positioning at present DAR.

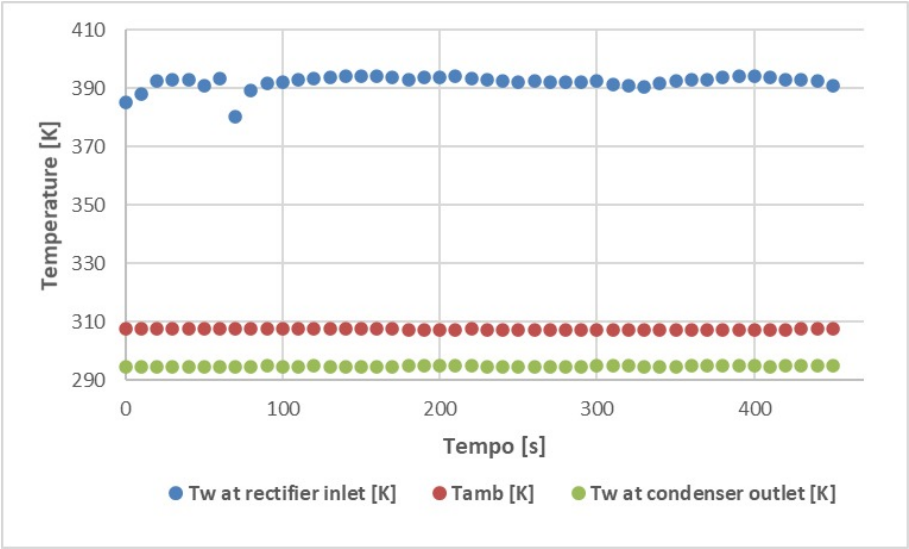

Figure 5: Thermocouples measurements.

average surface emissivity equals 0.99.

3.2 Model input variables values

The known model input variables values are shown Tab. 1

3.3 Generator and rectifier models

It was found from this model that for pressures greater than $2.02.10^6$ Pa ammonia condensation starts in rectifier. Then, it was necessary to determine three polynomials to compose condenser model: ($\dot{m}_1$), Eq. (17), (h_1), Eq. (18) or Eq. (19), and rectifier remaining length where ammonia condensation may occur (Lr_{rect}), Eq. (20), all as pressure function (P). For pressures lower than $2.02.10^6$ Pa, Lr_{rect} is null and L_{cond} is fixed. These functions were obtained from a parametric table construction in EES followed by curve interpolation.

$$\dot{m}_1 = 3.04986.10^{-12}P + 3.14828.10^{-5} \tag{17}$$

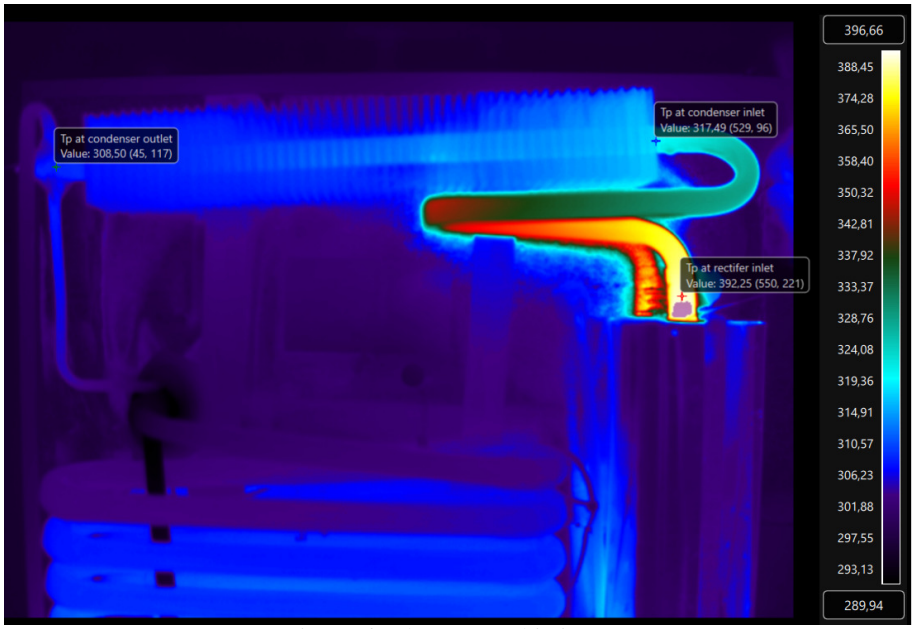

Figure 6: Thermographic image.

Table 1: Values of models input variables.

Generator/rectifier model		Siphon model		Condenser model	
Variable	Value	Variable	Value	Variable	Value
$D_{rectext}$, mm	14.7	L_s, m	1	L_{cond}, m	0.33
$D_{rectint}$, mm	11.7			θ, °	4
$\dot{Q}_{gen}$, W	80.7			$D_{condint}$, mm	10.65
L_{rect}, m	0.45	D_s, mm	1.08	$D_{condext}$, mm	14.65
P_{atm}, Pa	91			η_{fin}, dimensionless	0.9
T_{amb}, °C	21.7	D_s, mm	1.08	$S_{eachfin}$, m^2	0.0033
ϵ, dimensionless	0.99				
x_7, dimensionless	0.30	K, dimensionless	7	N_{fin}, dimensionless	54
$\dot{m}_7$, kg/s	5E-4				

$$h_1 = f(P, T_1) = f(P, 1.89482.10^{-11}P^2 - 4.63510.10^5 P + 339.587), P \leq 2.02.10^6 \tag{18}$$

$$h_1 = f(P, q = 0), P > 2.02.10^6 \tag{19}$$

$$Lr_{rect} = -3.78633.10^{-15}P^2 + 1.15375.10^{-8}P + 0.277218, P > 2.02.10^6 \tag{20}$$

3.4 Siphon model

Figure 7 shows condenser inlet and outlet mass flow rates obtained by generator/rectifier and siphon models, respectively. It should be noted that $\dot{m}_2$ curve was plotted for saturated liquid condition. Reynolds number for any operating pressure is less than 2300, which confirms a laminar flow always.

3.5 Condenser model

After loop calculations the system total operating pressure obtained was 1477000 Pa. This means that there has been no ammonia condensation yet in rectifier. Also, there has been a small subcooling at condenser. Therefore, the main results for the convergence pressure obtained are: $\dot{Q}_{cond}$ equals 40.1 W, T_w at rectifier inlet, T_1, T_2, T_w at condenser inlet and T_w at condenser outlet are equal to 368.2 K, 311.3 K and 311.1 K, 311.1 K and 311.0 K. These results represent

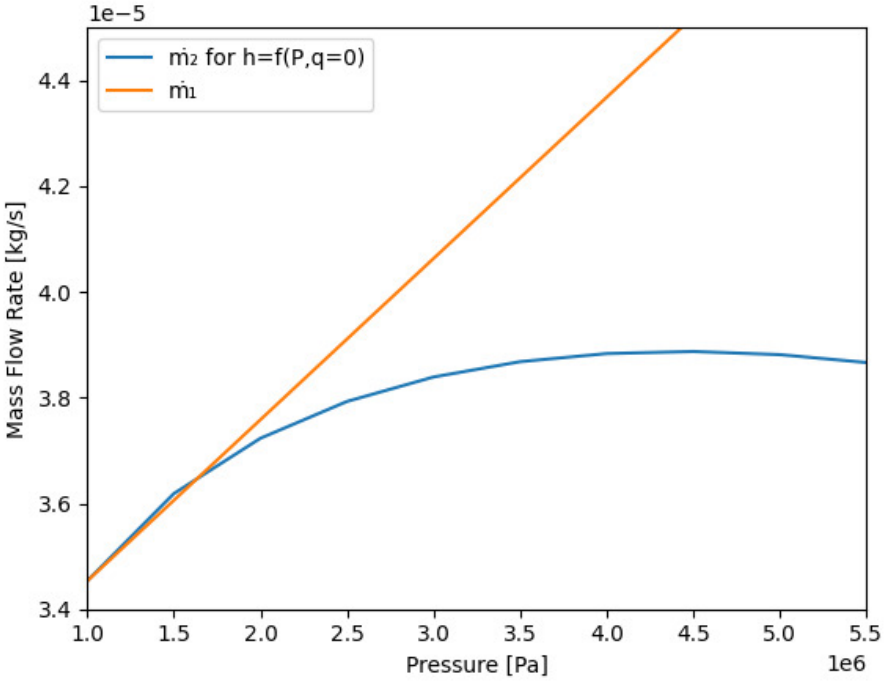

Figure 7: Condenser inlet and outlet mass flow rates.

percentage differences of approximately 6.1%, 1.2%, and 2.0% with respect to thermocouples experimental data for T_w at rectifier inlet, T_w at condenser inlet and T_w at condenser outlet, respectively, which shows good prediction of the present model. Since T_1 and T_2 are nearly identical and T_1 equals saturated temperature for the convergence pressure obtained, the aforementioned small subcooling is noticed. Futhermore, Fig. 8a shows ammonia and wall temperature profiles in condenser and Fig. 8b shows ammonia quality and void fraction, useful for mass calculating in condenser.

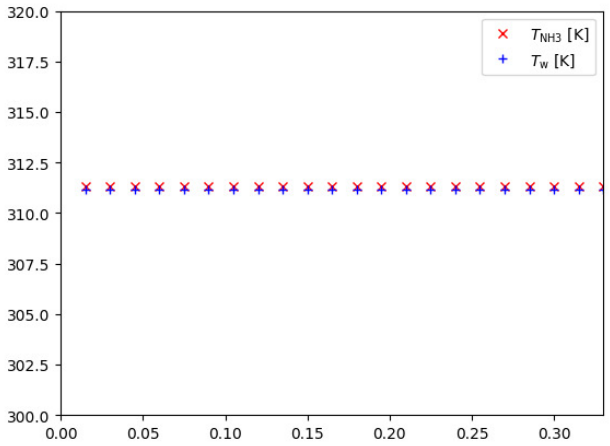

(a) Ammonia and wall temperature profiles in condenser.

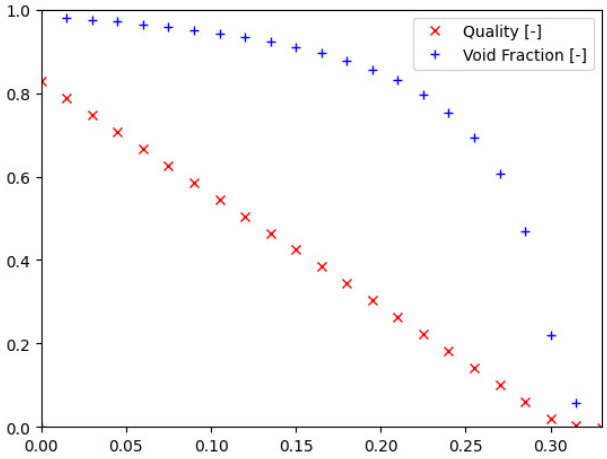

(b) Ammonia quality and void fraction.

Figure 8: Condenser profiles.

4. CONCLUSIONS

The main objective of this work was to develop a distributed steady state condenser model of a commercial $H_2O/NH_3/H_2$ diffusion absorption refrigerator that will be used for vaccines storage in regions without electrification by replacing the electrical resistance with a parabolic cylindrical solar collector for heat a thermal oil, a secondary fluid that will exchange heat with ammonia/water solution. For this, generator and siphon mathematical models also needed to be developed to determine the system total operating pressure by means of a mass balance. Generator model was developed in EES and the necessary polynomial results were obtained for integrate condenser and siphon models, both developed in Python language. Generator input mass flow rate and output mass concentration, data from other DAR components, needed to

be estimated to compose generator model. Parametric tables constructed in EES have shown that varying these parameters does not significantly change the values of the output variables, which enable a coherent development of the present model. The system total operating pressure obtained was 1477000 Pa. For this pressure, wall temperatures in three important points were calculated and it showed a difference of maximum 6.1% compared to experimental values, obtained by thermographic and thermocouples measurements. Hence, the present model predicts with good accuracy the refrigerator steady state behavior and the other components modeling can continue in elaboration to complete full cycle modeling.

5. ACKNOWLEDGEMENTS

The authors would like to thank the National Council for Scientific and Technological Development (CNPq in Portuguese), the Improvement Coordination of Higher Education Personnel (CAPES in Portuguese), the Foundation for Research Support of the Minas Gerais State (FAPEMIG in Portuguese) and the Multiuser Scientific Thermography Center of Federal University of Minas Gerais (CEMTEC-UFMG in Portuguese).

6. REFERENCES

Alvala, R.C.S., Dias, M.C.A., Saito, S.M., Stenner, C., Franco, C., Amadeu, P., Ribeiro, J., Santana, R.A.S.M. and Nobre, C.A., 2019. "Mapping characteristics of at-risk population to disasters in the context of brazilian early warning system". *International Journal of Disaster Risk Reduction*, Vol. 41.

Chaves, F.D., Moreira, M.F.S., Koury, R.N.N., Machado, L. and Cortez, M.F.B., 2019. "Experimental study and modelling within validation of a diffusion absorption refrigerator". *International Journal of Refrigeration*, Vol. 101, pp. 136–147.

Choi, H.W., Lee, J.W. and Kang, Y.T., 2022. "Experimental study on diffusion absorption refrigerator achieving 0.2 coefficient of performance using low global warming potential refrigerant and low-grade heat source". *Applied Thermal Engineering*, Vol. 201.

IEA, 2022. "For the first time in decades, the number of people without access to electricity is set to increase in 2022". International Energy Agency, Paris, https://www.iea.org/commentaries/for-the-first-time-in-decades-the-number-of-people-without-access-to-electricity-is-set-to-increase-in-2022. Accessed 23 June 2023.

Incropera, F.R., Bergman, D.P.D.T.L. and Lavine, A.S., 2008. *Heat and mass transfer: fundamentals and applications*. Editora LTC, Rio de Janeiro.

Mansouri, R., Bourouis, M. and Bellagi, A., 2017. "Experimental investigations and modelling of a small capacity diffusion-absorption refrigerator in dynamic mode". *Applied Thermal Engineering*, Vol. 113, pp. 653–662.

Moreira, M.F.D.S., 2014. *Simulation Model of and Diffusion-Absorption Refrigerator Operating Under Transient Regime (in Portuguese)*. Ph.D. thesis, Graduate Program in Mechanical Engineering, Federal University of Minas Gerais, Belo Horizonte, Brazil.

Pérez-García, V., Rodríguez-Muñoz, J.L., Belman-Flores, J.M., Rubio-Maya, C. and Ramírez-Minguela, J.J., 2019. "Theoretical modeling and experimental validation of a small capacity diffusion-absorption refrigerator". *International Journal of Refrigeration*, Vol. 104, pp. 302–310.

Schmid, F., Bierling, B. and Spindler, K., 2019. "Development of a solar-driven diffusion absorption chiller". *Solar Energy*, Vol. 117, pp. 483–493.

Uddin, M.A., Mahmud, S., Salehin, S., Bhuiyan, M.A.A., Riaz, F., Modi, A. and Salman, C.A., 2021. "Energy analysis of a solar driven vaccine refrigerator using environment-friendly refrigerants for off-grid locations". *Energy Conversion and Management*, Vol. 11.

Vasconcellos, G.L.F.D., 2019. *Energy Assessment of an Diffusion-Absorption Cooling System Driven by the Exhaust Gases of an Internal Combustion Engine (in Portuguese)*. Ph.D. thesis, Graduate Program in Mechanical Engineering, Pontifical Catholic University of Minas Gerais, Belo Horizonte, Brazil.

7. RESPONSIBILITY NOTICE

The authors are solely responsible for the printed material included in this paper.